P517607.PDF [Page: 3 of 33]

DEFENCE R&D DÉFENSE

# Analysis of Multipath Interference for SAR Countermeasures Trials

P. Sévigny

**Defence R&D Canada**
TECHNICAL MEMORANDUM
DREO TM 2001-106
January 2002

National Defence Défense nationale

Canada

105-03213/

# REPRODUCTION QUALITY NOTICE

This document is the best quality available. The copy furnished to DRDCIM contained pages that may have the following quality problems:

: Pages smaller or Larger than normal

: Pages with background colour or light coloured printing

: Pages with small type or poor printing; and or

: Pages with continuous tone material or colour photographs

Due to various output media available these conditions may or may not cause poor legibility in the hardcopy output you receive.

☒ If this block is checked, the copy furnished to DRDCIM contained pages with colour printing, that when reproduced in Black and White, may change detail of the original copy.

# Analysis of Multipath Interference for SAR Countermeasures Trials

P Sévigny
Defence Research Establishment Ottawa

**Defence Research Establishment Ottawa**
Technical Memorandum
DREO TM 2001-106
January 2002

Author

P. Sévigny

Approved by

B Bridgewater
Head/ECM

Approved for release by

G Marwood
Head/Document Review Panel

© Her Majesty the Queen as represented by the Minister of National Defence, 2002
© Sa majesté la reine, représentée par le ministre de la Défense nationale, 2002

## Abstract

This document presents a model developed to study the impact of multipath interference on jammer performance during Electronic Counter-Measures (ECM) trials against Synthetic Aperture Radars (SARs) The work was motivated by the low grazing angle geometry of the NATO SCI-066 AhrCarSAR trial, where the SAR was driven on a long, high bridge while imaging the valley below

A simple model of specular reflection was used and analytical formulas were developed to make predictions It was found that the geometry of the AhrCarSAR trial was subject to multipath interference, as are some airborne geometries as well The analysis of the model showed that the interference of direct and reflected-path pulses results in a chirp with a power modulation determined mainly by the reflection coefficient of the surface near the jammer For horizontal polarizations, the reflection coefficient approaches 1 and multipath effects can be important For vertical polarizations however, the reflection coefficient can be significantly less than 1 and multipath effects are weak Since a vertical polarization is used for the AhrCarSAR trial, it was predicted that the performance of the jammer would not be significantly affected by multipath interference

## Résumé

Ce document présente un modèle développé pour étudier l'impact de l'interférence due à la propagation par trajets multiples sur la performance d'un brouilleur lors d'essais de contre-mesures électroniques contre les radars à antenne synthétique (SAR) Ces travaux étaient motivés par la géométrie particulière utilisée lors des essais AhCarSAR organisés par le groupe NATO SCI-066, où le SAR est installé sur une voiture qui roule sur un pont haut et long, tout en faisant l'image de la vallée au-dessous à l'aide d'un petit angle d'arrivée au sol

Un modèle simplifié de réflexion spéculaire a été utilisé et des formules analytiques ont été développées afin de faire des prédictions Il en a résulté que les essais AhrCarSAR, ainsi que certaines autres géométries contre les SAR aéroportés, étaient sujets à de l'interférence due à la propagation par trajets multiples L'analyse a démontré que l'interférence entre les fluctuations de longueur d'onde (chirp) des faisceaux direct et réfléchi résultait en une fluctuation de longueur d'onde semblable mais avec une modulation de l'enveloppe déterminée principalement par le coefficient de réflexion de la surface près du brouilleur Pour une polarisation horizontale, le coefficient de réflexion approche la valeur de 1, et les effets d'interférence due à la propagation par trajets multiples sont importants Pour une polarisation verticale par contre, le coefficient de réflexion est peu élevé et les effets d'interférence due à la propagation par trajets multiples sont faibles Puisqu'une polarisation verticale est utilisée pour les essais AhrCarSAR, il a été prédit que la performance du brouilleur ne serait pas affectée

de façon significative par l'interférence due à la propagation par trajets multiples

P517607.PDF [Page: 9 of 33]

## Executive summary

The Electronic Countermeasures (ECM) Section of the Defence Research Establishment in Ottawa (DREO) is conducting research in countermeasures against Synthetic Aperture Radar (SAR) systems installed on elevated platforms using a jammer positioned on the ground. As part of this research program, the NATO SCI-066 AhrCarSAR field trial was recently organized to test ECM techniques in a controlled environment. This trial was unique in that the SAR was mounted on a van and was driven on a long, high bridge while imaging the valley below with a very low grazing angle. The jammer was positioned in a parking lot in the valley, within the area imaged by the SAR. The jammer captured the SAR pulses in order to repeat them with delays and modulations appropriate for the intended ECM techniques.

During the planning phase of the trial, it was identified that the performance of the jammer could possibly be affected by the multipath interference expected with the low grazing angle geometry of the trials. A simple model of specular reflection was thus used and analytical formulas were developed to predict the impact of multipath interference on the jammer performance.

As expected, the analysis conducted showed that the AhrCarSAR geometry was susceptible to multipath interference, but also that other airborne geometries could face the same problem. It was further determined that, in general, the SAR pulses following the path reflected on the ground arrive with a delay relative to the SAR pulses following the direct path, and that the delay was very short compared to the SAR pulse width. As a result, the direct-path and the reflected-path pulses can be considered to interfere at the jammer antenna for the entire pulse duration. The result of the interference is a similar pulse except that the power envelope shows a modulation.

It was also shown that the value of the reflection coefficient of the ground near the jammer determines the amplitude of the power modulation. For vertical polarizations, the reflection coefficient can be significantly less than 1 and the multipath interference is weak. For horizontal polarizations however, the reflection coefficient is close to 1 and strong multipath interference can be expected.

The results indicate that for the AhrCarSAR trial parameters and geometry, multipath interference would not significantly affect the jammer performance, except for a slight decrease in received power. The model developed was shown to be useful for planning the experimental setup, and helped in predicting received powers. In fact, the generality of the model developed will allow other geometries to be studied, when required.

P. Sévigny; 2002; Analysis of Multipath Interference for SAR Countermeasures Trials; DREO TM 2001-106; Defence Research Establishment Ottawa

## Sommaire

La section des Contre-Mesures Électroniques (CME) du Centre de Recherches pour la Défense à Ottawa (CRDO) étudie les contre-mesures contre les radars à antenne synthétique (SAR) installés sur des plate-formes élevées, en utilisant un brouilleur placé au sol. Dans le cadre de ce programme de recherche, les essais AhrCarSAR furent organisés récemment pour tester des techniques de contre-mesures dans un environnement contrôlé. Ces essais avaient la particularité d'utiliser le SAR alors qu'il était installé sur une voiture qui roulait sur un pont haut et long, tout en faisant l'image de la vallée au-dessous à l'aide d'un petit angle d'arrivée au sol. Le brouillleur était positionné dans une aire de stationnement dans la vallée, et ce à l'intérieur de la surface imagée par le SAR. Le brouilleur faisait la saisie des pulses du SAR pour ensuite répéter ces pulses avec des délais et des modulations qui répondaient aux objectifs des techniques de contre-mesures.

Pendant la phase de planification des essais, la question de l'interférence due à la propagation par trajets multiples fut abordée. En fait, avec le petit angle au sol des essais, il était anticipé qu'il y aurait de l'interférence due à la propagation par trajets multiples, et l'impact de cette interférence était inconnu. Un modèle simple de réflexion spéculaire fut alors utilisé et des formules analytiques furent dévelopées pour prédire l'impact de l'interférence due à la propagation par trajets multiples sur la performance du brouilleur.

L'analyse a montré que la géométrie des essais AhrCarSAR était effectivement sujette à des problèmes d'interférence, comme il était anticipé, mais que d'autres géométries avec le SAR aéroporté pourraient subir les mêmes difficultés. Les calculs montrent que les pulses suivant le faisceau réfléchi sur le sol arrivent au brouilleur avec un délai comparativement aux pulses suivant le faisceau direct, et que ce délai est très court par rapport à la largeur du pulse. Avec ce résultat, on peut considérer que les pulses réfléchi et direct interfèrent en entier à leur arrivée à l'antenne du SAR. Le résultat de l'interférence est donc un pulse rectangulaire sauf que l'enveloppe du pulse est modulée.

Il a été montré également que la valeur du coefficient de réflexion du sol près du brouilleur détermine l'amplitude de la modulation du pulse. Pour des polarisations verticales, le coefficient de réflexion est faible et l'interférence est faible. Pour des polarisations horizontales par contre, le coefficient de réflexion est près de 1 et beaucoup d'interférence doit être anticipée.

Les résultats indiquent que pour les paramètres et la géométrie des essais AhrCarSAR, l'interférence due à la propagation par trajets multiples n'aurait pas d'impact significatif sur le brouilleur, sauf pour une faible atténuation de la puissance détectée. Le modèle developé fut utile pour la planification des expériences, et a aidé à prédire la puissance détectée. En fait, la généralité du modèle développé permettra d'étudier d'autres géométries, au besoin.

P Sévigny 2002. Analyse de l'Interférence due à la Propagation par Trajets Multiples dans le Contexte d'Essais de Contre-Mesures contre les SAR DREO TM 2001-106 Centre de recherches pour la défense Ottawa

# Table of contents


Abstract . . . . . i

Résumé . . . . . i

Executive summary . . . . . iii

Sommaire . . . . . iv

Table of contents . . . . . vi

List of figures . . . . . vii

List of tables . . . . . vii

1 Introduction . . . . . 1

2. Geometry of SAR countermeasures trials . . . . . 2

2.1 Generic geometry for SAR countermeasures trials . . . . 2

2.2 Criterion for multipath interference . . . . . 2

2.3 Reflection point on the ground . . . . . 4

2.4 Range difference between direct and reflected paths . . 4

3. Effect of multipath interference on the jammer performance . . . . . 6

3.1 Reflection of an RF pulse on the ground . . . . . 6

3.2 Interference of two chirp waveforms . . . . . 7

3.3 Interference of the direct-path pulse and the reflected pulse . 8

3.4 Mean power of the interference pulse . . . . . 9

3.5 Time history of the jamming pulses . . . . . 10

4 Conclusions . . . . . 15

References . . . . . 16

P517607.PDF [Page: 13 of 33]

## List of figures


| | | |
|---|---|---|
| 1 | Generic SAR countermeasures trial geometry | 2 |
| 2 | SAR countermeasures trial geometry, for $R_{dn} \gg h_j$ | 3 |
| 3 | Spaceborne, airborne, and car configurations for which multipath interference is expected | 5 |
| 4 | Power density envelope of the interference pulse for range delays of 2 m and 19 cm | 11 |
| 5 | Illustration of the finite size of the jammer antenna | 12 |
| 6 | Mean power versus time delay | 12 |
| 7 | Mean power versus distance jammer-SAR | 13 |
| 8 | Mean power detected at the jammer antenna as a function of time for the AhrCarSAR trial geometry | 14 |


## List of tables


| | | |
|---|---|---|
| 1 | Geometry parameters for the AhrCarSAR trial | 4 |
| 2 | Parameters of the AhrCarSAR trial | 8 |

# 1. Introduction

In the past several years, the Electronic Countermeasures (ECM) Section of Defence Research Establishment Ottawa (DREO) has been conducting research in countermeasures against SAR systems installed on elevated platforms using a jammer positioned on the ground. As part of this research program and in collaboration with the NATO SCI-066 Task Group (TG 13), the AhrCarSAR field trial was recently organized in Germany to test ECM techniques in a controlled environment. This trial was unique in that the SAR system was mounted on a van and was driven on a long and high bridge while imaging the valley below with a very low grazing angle, or equivalently, a very high incidence angle.

During the trial planning, a question was raised about the effect of multipath interference on the jammer performance. Multipath is a well-known problem for detection at low grazing angles, for example when an aircraft navigating below a given altitude cannot be detected by a search radar due to the coherent interference between direct and reflected-path radar beams[1, 2]. However, SARs commonly use chirp waveforms, and multipath interference in this case is not well documented. Furthermore, in the case of SAR ECM trials, it is desirable to study the effect of multipath at a specific point in space, i.e. at the jammer location. In particular, it is useful to predict the shape of the detected pulses in order to evaluate whether jammer detection and acquisition tasks can be perturbed by multipath interference. If multipath interference is found to be problematic at the jammer location for SAR ECM trials, it is also expected to affect SAR processing of the jamming signals, but the analysis of this effect is beyond the scope of this paper.

This paper presents some analysis and modelling of multipath for counter-SAR trials in general and some calculations for the AhrCarSAR geometry and parameters in particular. Section 2 presents the model used for the geometry of counter-SAR trials, while Section 3 develops the model for the multipath interference at the jammer antenna. Finally, Section 4 draws some conclusions about this work.

# 2. Geometry of SAR countermeasures trials

In this section, the generic geometry for SAR countermeasures trials is presented in 2.1, a criterion for the existence of multipath interference is established in 2.2, the distance between the jammer and the reflection point on the ground is calculated in 2.3, and the range difference between direct and reflected beams is determined in 2.4.

## 2.1 Generic geometry for SAR countermeasures trials

Figure 1 illustrates the basic geometry of a SAR countermeasures trial setup, assuming the ground is a flat-earth plane reflector. The radar progresses along its line of flight at an altitude of $h_r$ above the ground, and the jammer is placed at a (typically) low height $h_j$. The radar nadir point (i.e. the point on the surface of the Earth directly below the radar) and the jammer are separated by a ground range $r_g$. The range between the jammer and the radar is indicated as $R_{dir}$, while $R_{refl}$ indicates the reflected path. $\theta_1$ and $\theta_2$ are the angles between the horizontal and the direct and the reflected paths respectively. The ground distance between the jammer and the reflection point on the ground is indicated as $d$ in the figure. The dashed lines below the Earth surface help visualize the specular reflection.

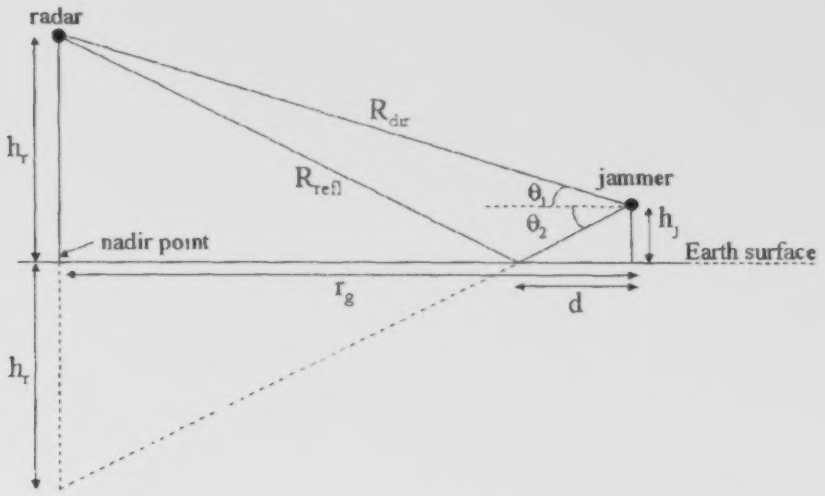


***Figure 1:*** *Generic SAR countermeasures trial geometry*

## 2.2 Criterion for multipath interference

For the simple analysis presented here, multipath interference is assumed to occur if both the direct and the reflected beams are within the mainlobes of both the jammer and

the radar antennas. To determine if this criterion is met, basic geometry equations can be derived, as follows

First, it is assumed that the radar is pointing in a way such that the jammer is within its mainlobe. The sidelobes will not be considered here. In other words, only the time when the jammer is within the footprint of the radar is of interest. It is also assumed that the jammer antenna is pointing at the elevation of the radar, i.e. is centered on the direct path, and in azimuth at the point of closest approach of the radar.

Second, if $R_{dir} \gg h_j$, the direct and reflected beams can be considered parallel as illustrated in Fig. 2, and we can assume that $\theta_1 = \theta_2 = \theta$. In this particular case, the reflected beam is assumed within the radar main beam, and is within the jammer main beam if

$$\frac{1}{2}\phi_j \geq 2\theta, \tag{1}$$

or

$$\phi_j \geq 4\arctan\left(\frac{h_r - h_j}{r_g}\right). \tag{2}$$

where $\phi_j$ is the jammer antenna elevation beamwidth

***Figure 2:*** *SAR countermeasures trial geometry, for $R_{dir} \gg h_j$*

Figure 3 illustrates this condition by graphing the radar altitude $h_r$ versus the ground range $r_g$. The figure was generated using a jammer antenna elevation beamwidth of 60° and a jammer height of 1 m. The gray zones represent the configurations where multipath interference is expected to be present. Plots (b) and (c) are a zoom of plot (a) for airborne and car geometries. It can be seen that for typical spaceborne geometries ($h_r \sim 800$ km), no multipath interference is expected. For car geometries however, multipath interference will be present for any jammer location and radar/bridge height. For airborne geometries ($h_r \sim 3 - 6$ km), multipath interference can occur, especially at large ranges (low grazing angles)

## 2.3 Reflection point on the ground

The distance $d$ between the jammer and the reflection point on the ground can be calculated:

$$d = \frac{h_j}{\tan\theta} = \frac{h_j r_g}{h_t - h_j} \tag{3}$$

Table 1 presents the parameters of the AhrCarSAR trial, and these parameters will be used throughout this document. Using these parameters, the reflection point on the ground is at about 10.4 m in front of the jammer.

***Table 1:*** *Geometry parameters for the AhrCarSAR trial*

| | |
|---|---|
| $h_t$ | 66 m |
| $h_j$ | 1 m |
| $r_g$ | 674 m |

The model developed throughout this document assumes a flat-earth good specular reflector. In the case of the AhrCarSAR trial, the jammer is positioned in a flat parking lot in concrete, so this assumption is met. However, obstacles placed in the reflected path (at distances of 10-50 meters) can reduce or annihilate any multipath effect. For example, a car parked at 30 m in front of the jammer antenna would block the reflected path.

## 2.4 Range difference between direct and reflected paths

The range delay introduced by the reflection path can be calculated using geometry equations:

$$\begin{aligned} \delta_t &= R_{refl} - R_{dir} \\ &= \sqrt{(h_t + h_j)^2 + r_g^2} - \sqrt{(h_t - h_j)^2 + r_g^2} \end{aligned} \tag{4}$$

The jammer antenna is assumed to be aligned with the center of the bridge. From equation 4 and parameters of Table 1, the range difference is of about 19 cm (i.e. 18.3 cm when the radar is in the middle of the bridge, and 19.5 cm when the radar is at the end of the bridge). This range difference is equivalent to a delay of 0.65 ns. Comparing to a pulse width of $3\mu s$, we can assume that the reflected and direct-path pulses interfere for the whole pulse (i.e. there is no significant displacement of one pulse regarding the other one).

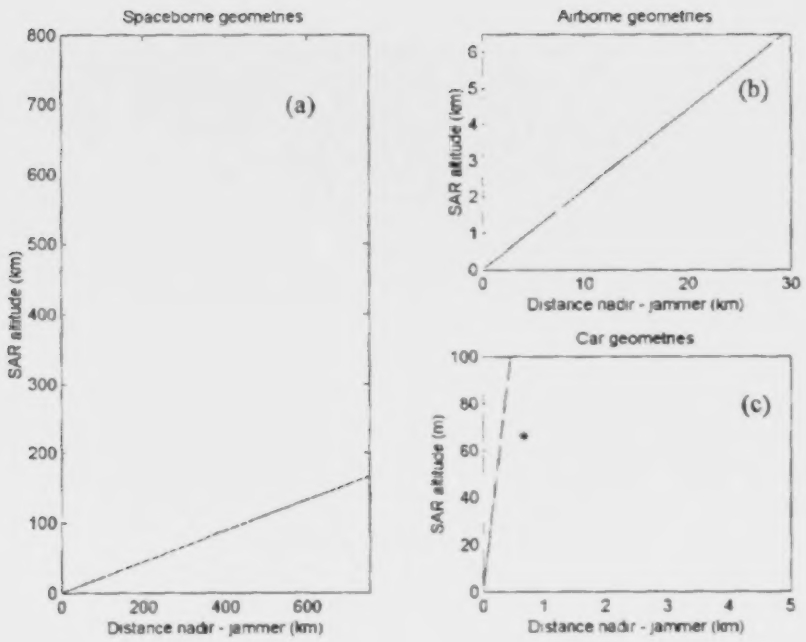


***Figure 3:*** *Spaceborne (a), airborne (b), and car (c) configurations for which multipath interference is expected. Gray zones represent configurations where the reflected beam on the ground enters the jammer main beam. The * symbol indicates the AhrCarSAR trial geometry. The jammer antenna elevation main beam was assumed to be 60°.*

# 3. Effect of multipath interference on the jammer performance

In this section, analytic formulas are developed to predict the shape and the power of the pulses detected at the jammer site. In 3.1, the model used for reflection of a radar pulse on the ground is presented, so that the interference of two chirp waveforms can be analysed in 3.2 and 3.3. Some more analysis is presented on the mean power detected as a function of the jammer position (3.4) and as a function of the position of the radar on the bridge (3.5).

## 3.1 Reflection of an RF pulse on the ground

When an electromagnetic wave is reflected at any interface between two different materials, the difference of dielectric properties of the two materials induce an attenuation and a phase shift to the wave. In the case of the AhrCarSAR trial discussed here, reflection occurs at very low grazing angles (of about 6°) over a flat concrete parking lot. For horizontal polarization, the RF is not attenuated but the phase is shifted by 180°. For a vertical polarization, ref. [3] reports measurements of reflection coefficients and phase shifts over sea for a number of wavelengths. For the AhrCarSAR trial, since the parking lot can be assumed to be a good specular reflector, the following parameters of the sea will be used for the calculations: 0.2 for the reflection coefficient and 150° for the phase shift, for $\theta = 6°$, in agreement with good ground data reported in [1].

If the direct-path pulse amplitude at the jammer is of the form

$$V_{dir} = V_0 e^{i2\pi f(t)t} \qquad t \leq |\tau_p/2| \tag{5}$$

where $V_0$ is the amplitude per unit area, $f(t)$ the frequency and $\tau_p$ the pulse width, then the reflected pulse is:

$$\begin{aligned} V_{ref} &= \rho_0(\theta) V_{dir}(t - \delta_t) e^{i\phi(\theta)} && -\frac{\tau_p}{2} + \delta_t \leq t \leq +\frac{\tau_p}{2} + \delta_t \\ &= \rho_0(\theta) V_0 e^{i(2\pi f(t-\delta_t)(t-\delta_t) + \phi(\theta))} && -\frac{\tau_p}{2} + \delta_t \leq t \leq +\frac{\tau_p}{2} + \delta_t \end{aligned} \tag{6}$$

where $\rho_0(\theta)$ is the reflection coefficient, $\phi(\theta)$ the phase shift, and $\delta_t$ the time delay between pulses introduced by the different paths. For the remaining of this document, $\delta_t$ will be neglected in the definition of the formulas, so that both $V_{ref}$ and $V_{dir}$ will be defined for $t \leq |\tau_p/2|$. This assumption is acceptable for the short time delays expected (see Section 2.4). The requirement $t \leq |\tau_p/2|$ will also be assumed in what follows.

## 3.2 Interference of two chirp waveforms

Considering both SAR and jammer antennas as points in space, the interference of the reflected and direct pulses can be described analytically. Following equations 5 and 6:

$$\begin{aligned} V_{tot}(t) &= V_{dir}(t) + V_{ref}(t) \\ &= V_0 e^{i2\pi f(t)t} + \rho_0(\theta) V_0 e^{i(2\pi f(t-\delta_t)(t-\delta_t) + \phi(\theta))} \end{aligned} \tag{7}$$

As will be demonstrated shortly, $V_{tot}$ at any time $t$ is the superposition of two waves, with an instantaneous frequency offset of $f(t) - f(t-\delta_t)$ and a phase offset $\phi(\theta)$. This superposition results in a beat pattern. Of course in the case of a constant frequency signal, the frequency offset is zero and only the phase offset $\phi(\theta)$ determines if the waves are interfering destructively or constructively. In the case of a chirp, the resulting pulse is similar to the original chirp but the envelope of the pulse is modulated according to the beat pattern. In the case of a chirp with linear frequency modulation, the modulation depends only upon the pulse width, the bandwidth, and the time delay. In the case of non-linear frequency modulation, the modulation can take a more complex pattern.

To keep the discussion general, we will consider the frequency of the chirp to be of the form

$$f(t) = f_0 - \frac{\beta}{\pi} t - \gamma t^2. \tag{8}$$

where the bandwidth of the chirp is equal to $\frac{\beta \tau_p}{\pi}$. Note that for a linear frequency modulation (LFM) chirp, $\gamma = 0$.

Using the fact that

$$f(t-\delta_t) = f_0 - \frac{\beta}{\pi}(t-\delta_t) - \gamma(t-\delta_t)^2 = f(t) + \frac{\beta}{\pi}\delta_t + 2\gamma t\delta_t - \gamma\delta_t^2. \tag{9}$$

Equation 7 becomes

$$\begin{aligned} V_{tot} &= V_0 e^{i2\pi f(t)t} + \rho_0(\theta) V_0 e^{i(2\pi f(t-\delta_t)(t-\delta_t) + \phi(\theta))} \\ &= V_0 e^{i2\pi f(t)t} \left\{ 1 + \rho_0(\theta) e^{i\phi(\theta)} e^{i2\pi\left[\frac{\beta}{\pi}\delta_t + 2\gamma t\delta_t - \gamma\delta_t^2\right]t} e^{-i2\pi\left[f_0 - \frac{\beta}{\pi}t - \gamma t^2 + \frac{\beta}{\pi}\delta_t + 2\gamma t\delta_t - \gamma\delta_t^2\right]\delta_t} \right\} \\ &= V_0 e^{i2\pi f(t)t} \left\{ 1 + \rho_0(\theta) e^{i\phi(\theta)} e^{i2\pi 3\gamma\delta_t t^2} e^{i2\pi\left[2\frac{\beta}{\pi}\delta_t - 3\gamma\delta_t^2\right]t} e^{-i2\pi\left[f_0\delta_t + \frac{\beta}{\pi}\delta_t^2 - \gamma\delta_t^3\right]} \right\} \end{aligned} \tag{10}$$

From the last equation, we can appreciate that the interference chirp signal is modulated in time by the term in parentheses. The power density envelope is given by

$$\begin{aligned} I(t) &= V_{tot}^* V_{tot} \\ &= V_0^2 \Big\{ 1 + \rho_0(\theta)^2 + 2\rho_0(\theta) \times \\ &\cos\left(6\pi\gamma\delta_t t^2 + \left[4\beta\delta_t - 6\pi\gamma\delta_t^2\right] t - \left[2\pi f_0\delta_t + 2\beta\delta_t^2 - 2\pi\gamma\delta_t^3\right] + \phi(\theta)\right) \Big\} \end{aligned} \tag{11}$$

The value of the reflection coefficient $\rho_0(\theta)$ determines the smoothness of the power density modulation, and the phase shift $\phi(\theta)$ determines the phase of the power density modulation.

#### Chirp with linear frequency modulation

For an LFM chirp, $\gamma = 0$ and the interference chirp waveform and power density envelope simplify to,

$$V_{tot} = V_0 e^{i2\pi f(t)t} \left\{ 1 + \rho_0(\theta) e^{i\phi(\theta)} e^{i4\beta\delta_t t} e^{-i2\pi\left[f_0\delta_t + \frac{\beta}{\pi}\delta_t^2\right]} \right\} \quad (12)$$

$$I(t) = V_0^2 \left\{ 1 + \rho_0(\theta)^2 + 2\rho_0(\theta)\cos\left(4\beta\delta_t t - \left[2\pi f_0\delta_t + 2\beta\delta_t^2\right] + \phi(\theta)\right) \right\} \quad (13)$$

Figure 4 (a) illustrates the power density envelope of this beat pattern for a time delay $\delta_t$ corresponding to a range difference of 2 m. This large range difference was chosen to clearly show the beat pattern. Figure 4 (b) illustrates the pattern for the geometry of the AhrCarSAR trial, with a range difference of 0.19 m. The graphs were produced with the parameters listed in Table 2.

For the AhrCarSAR trial geometry, the beat frequency (given by the term $4\beta\delta_t t$) is low and the power density envelope does not show many cycles of the modulation, which avoids complications for the jammer acquisition. It can thus be predicted that the detected interference pulse would be of a chirp type exactly like the direct-path pulse, except for power attenuation or amplification.

## 3.3 Interference of the direct-path pulse and the reflected pulse

The effect of the physical dimensions of the antennas on the interference pattern can now be examined. As a first approximation, it is assumed that all the direct-path rays entering the jammer antenna are practically parallel, since the diameters of both SAR and jammer antennas are much smaller than the range between the antennas, as illustrated in Figure 5. If the jammer antenna is pointed at the SAR, then the power

***Table 2:*** *Parameters of the AhrCarSAR trial*

| | | | |
|---|---|---|---|
| SAR parameters | Frequency | $f_0$ | 10 GHz |
| | Bandwidth | $\frac{\beta\tau_p}{\pi}$ | 160 MHz |
| | LFM waveform | $\gamma$ | 0 |
| | Pulse width | $\tau_p$ | $3\mu s$ |
| | Polarization | | VV |
| Geometry parameters | Grazing angle | $\theta$ | 6° |
| Reflection parameters | Reflection coefficient | $\rho_0(\theta)$ | 0.2 |
| | Phase shift | $\phi(\theta)$ | 150° |

received from the direct path is a function of the antenna gain (for a 0 degrees angle) and of the antenna aperture size

For the reflected path, all beams can be assumed to be in phase at the entrance of the antenna. The inclination of the antenna relative to the reflected path causes some phase cancellation, which is due to the antenna gain in the direction of the reflected beam. Furthermore, a smaller effective aperture is seen by the reflected beams. Overall, the power density given by equation 13 can be rewritten as the detected power

$$P(t) = V_0^2 \Big\{ G(0^o) A_e + G(2\theta) A_e \sin\Omega \rho_0(\theta)^2 + 2\sqrt{G(0^o)G(2\theta)\sin\Omega} A_e \rho_0(\theta) \cos\left( 4\pi \frac{\beta}{\pi} \delta_t t - 2\pi \left[ f_0 \delta_t + \frac{\beta}{\pi} \delta_t^2 \right] + \phi(\theta) \right) \Big\} \quad (14)$$

where $G(0^o)$ and $G(2\theta)$ are the antenna gains in the pointing angle direction and the reflected path direction respectively, and $\sin\Omega = \sin(\pi/2 - 2\theta)$ is the antenna aperture reduction factor

Equation 14 shows that the finite size of the jammer antenna reduces the power modulation of the received chirp. Therefore the curves illustrated in Figures 4 (a) and (b) would be smoother if the effect of the antenna size and pattern was included. In this analysis, the earth is assumed a good specular reflector. In fact, more diffusion paths could enter the jammer antenna. This effect is believed to be negligible and would likely smooth out the beat pattern even more

## 3.4 Mean power of the interference pulse

Since it has been shown that the shape of the interference pulse does not differ significantly from the direct pulse, at least for short delays between direct and reflected paths, the problem can be regarded from the perspective of the mean power detected for a single pulse. This allows the determination of distances from the radar where the received power is maximized or minimized in order to guide the placement of the jammer

In the case of an LFM chirp waveform, the mean power is

$$\begin{aligned} \overline{P} &= \int_{-\tau_p/2}^{+\tau_p/2} V_{tot} V_{tot}^* dt \\ &= V_0^2 \Big\{ G(0^o) A_e + G(2\theta) A_e \sin\Omega \rho_0(\theta)^2 \\ &+ \frac{\rho_0(\theta)\sqrt{G(0^o)G(2\theta)\sin\Omega} A_e}{2\beta\tau_p\delta_t} \sin(2\beta\delta_t\tau_p) \cos\left( \phi(\theta) - 2\pi \left[ f_0\delta_t + \frac{\beta}{\pi}\delta_t^2 \right] \right) \Big\} \end{aligned} \quad (15)$$

From the last equation, the mean power depends on the time delay between pulses $\delta_t$, and therefore depends on the range of the jammer to the SAR. In fact, a low-frequency

component is expressed by the sin term, while the cos term determines a high-frequency component. This is illustrated in Figure 6, where the mean power is shown over a wide range of time delays. This graph assumes that the grazing angle is kept constant, so that the reflection coefficient and the phase shift remain constant. The mean power can also be regarded as a function of the placement of the jammer. In the case of the AhrCarSAR trial however, since the altitude of the SAR is fixed, increasing time delays correspond to increasing ranges but decreasing grazing angles. If the variation of $\rho_0$ and $\phi$ with grazing angle is taken into account, the mean power at the jammer site can be calculated as a function of the ground range, as shown in Figure 7. For this graph, values of $\rho_0(\theta)$ and $\phi(\theta)$ were taken from [3], and the other parameters from Tables 1 and 2. For a distance of 674 m, the expected mean power, as calculated from Equation 15, is down by approximately 1.8 dB from the power of the direct-path pulse without interference.

## 3.5 Time history of the jamming pulses

Finally, the mean power detected at the jammer antenna as a function of time, i.e. as a function of the position of the SAR on the bridge is plotted in Figure 8. This graph was produced with a SAR platform velocity of 22.2 m/s and a range of 674 m. Time $t = 0$ corresponds to the case where the SAR is at its closest point of approach to the jammer, i.e. at the middle of the bridge in the case of the AhrCarSAR trial. The dashed line indicates the variation of the received power without multipath interference. The variation is due to the varying distance to the SAR. The solid line shows the variation of the received power with multipath interference, as given by Equation 15. It can be observed that as the SAR moves away from the closest point of approach (time $t = 0$), the distance to the jammer is increased, and the received power reaches a null at a distance of about 678 m (see Figure 7). For greater distances, the received power increases. The actual time of interest from the jammer point of view is only for a few seconds centered when the SAR is in the middle of the bridge, as indicated by the dashed lines of Figure 8. In this case, the power variation follows roughly the same curve than the direct-path pulse power, except for a power reduction of about 1.8 dB. The effect of the antenna pattern of both the SAR and the jammer was not illustrated in Figure 8, but would have the same impact on both cases, with and without multipath interference.

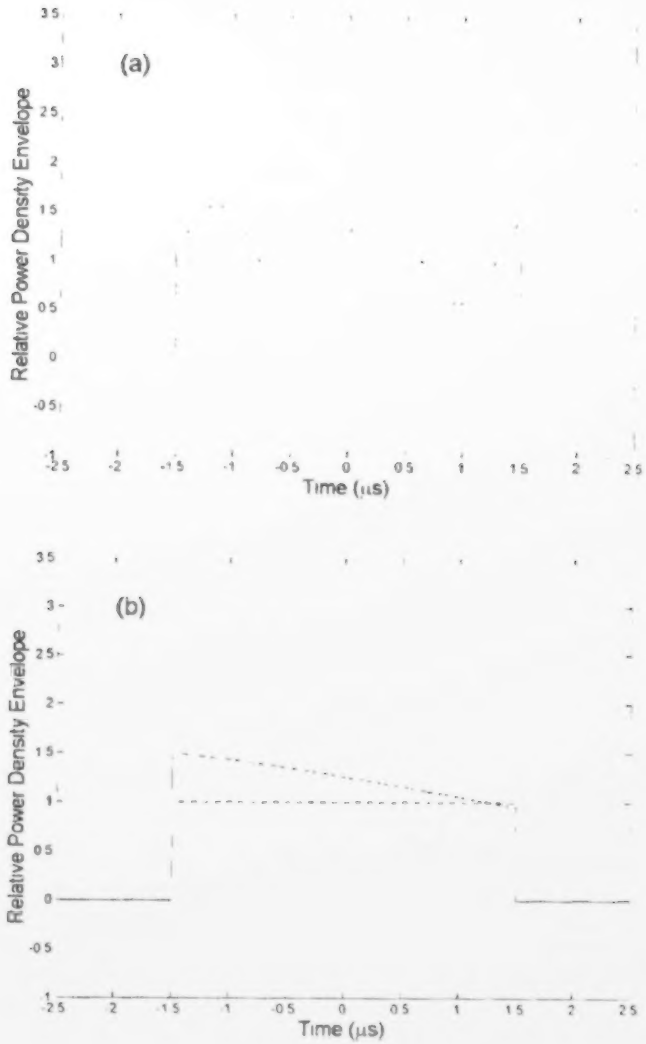


***Figure 4:*** *Power density envelope of the interference pulse for range delays of 2 m (a) and 19 cm (b) and a pulse width of 3μs. The power is relative to the direct-pulse power envelope, shown as the dashed line*

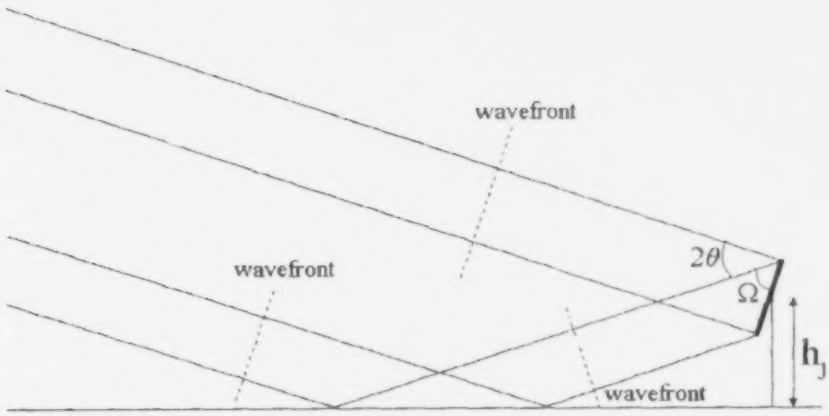


***Figure 5:*** *Illustration of the finite size of the jammer antenna*

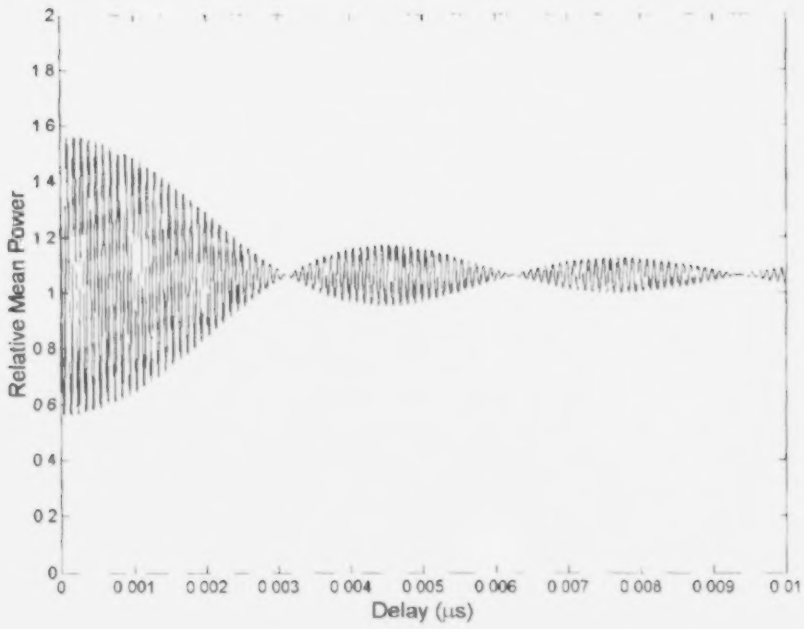


***Figure 6:*** *Mean power versus time delay The power is relative to the direct pulse mean power*

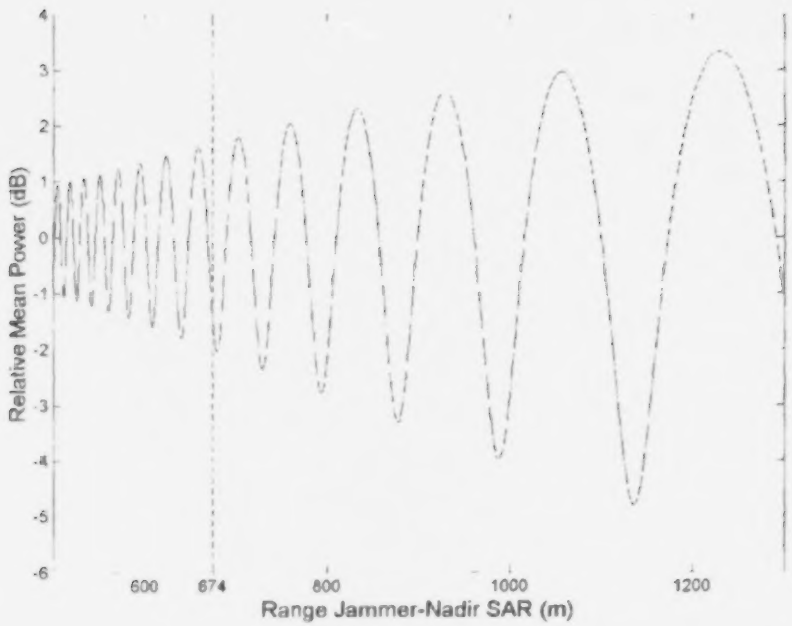


***Figure 7:*** *Mean power (in dB) versus the distance jammer-nadir SAR. The power is relative to the direct pulse mean power. The dashed line indicates the actual closest point of approach of the SAR to the jammer (at a range of 674 m) for the AhrCarSAR trial.*

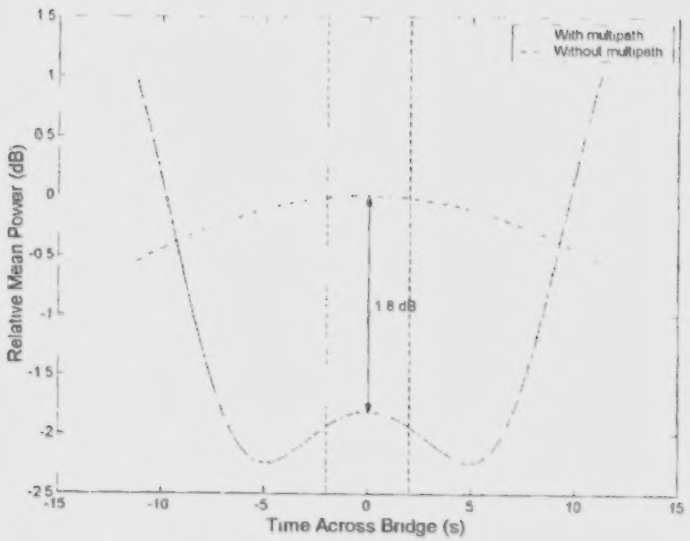


***Figure 8**: Mean power (in dB) detected at the jammer antenna as a function of time for the AhrCarSAR trial geometry. The dashed lines limit the time of interest from the jammer point of view. Within these boundaries, the received power with multipath interference follows roughly the same curve than the case without multipath interference, except for a power reduction of about 1.8 dB.*

# 4. Conclusions

In Section 2, equations were derived to determine geometries for which multipath interference at the jammer antenna can be expected. It was found that multipath is present for the AhrCarSAR trial geometry, but otherwise will not be commonly encountered. Only airborne counter-SAR trials with very low grazing angles are likely to be subject to multipath. In the presence of multipath interference, calculations show that the delay introduced by the reflected path is short compared to the pulse width, and so the reflected-path and direct-path pulses interfere almost entirely. Hence the time shift of one pulse with respect to the other one can be neglected.

In Section 3, the interference of the direct-path and the reflected-path pulses was modelled analytically using a simple model of specular reflection, where the reflected beam is attenuated by a factor $\rho_0(\theta)$ and shows a phase shift $\varphi(\theta)$. It follows that the interference pulse is a chirp with the same modulation as the original chirp, but with a phase offset and a power modulation. The amplitude of the power modulation depends on the attenuation factor $\rho_0(\theta)$, while the frequency of the modulation depends on the time delay introduced by the reflected path. The attenuation $\rho_0(\theta)$ plays a key role in the multipath effect. For vertical polarization, the reflection coefficient drops quickly when the grazing angle is augmented, and multipath interference is barely noticeable. For horizontal polarization however, the reflection coefficient approaches $\rho_0(\theta) = 1$ for all grazing angles, and multipath interference is expected to be more severe.

For the specific geometry of the AhrCarSAR trial, the presence of multipath interference was predicted. However, since a vertical polarization was used with a grazing angle of about 6°, the multipath effect was weak and a power reduction of about 1.8 dB was determined.

This paper presents results from the modelling and the analysis of multipath effects on the jammer performance in SAR countermeasures trials. Although this work was motivated by the very unusual geometry of the AhrCarSAR trial, where the SAR was mounted on a van and driven across a long and high bridge while imaging the valley below, the model developed is generic and can be applied for other geometries of SAR countermeasures trials, and possibly to other types of ECM trials.

P517607.PDF [Page: 30 of 33]

## References

1 Barton, B K., Cook, C. E , and Hamilton, P (1991) Radar Evaluation Handbook. Artech House.

2. Eaves, J L. and Reedy, E. K (1987) Principles of Modern Radar, Van Nostrand Reinhold Company

3 Skolnik, M I (1970). Radar Handbook, McGraw-Hill.

UNCLASSIFIED

SECURITY CLASSIFICATION OF FORM
(highest classification of Title, Abstract, Keywords)

## DOCUMENT CONTROL DATA

(Security classification of title, body of abstract and indexing annotation must be entered when the overall document is classified)

1 ORIGINATOR (the name and address of the organization preparing the document Organizations for whom the document was prepared, e g Establishment sponsoring a contractor's report, or tasking agency, are entered in section 8 )

DREO
3701 Carling
Ottawa, Ontario, K1A 0Z4

2 SECURITY CLASSIFICATION (overall security classification of the document, including special warning terms if applicable)

UNCLASSIFIED

3 TITLE (the complete document title as indicated on the title page Its classification should be indicated by the appropriate abbreviation (S,C or U) in parentheses after the title )

Analysis of Multipath Interference for SAR Countermeasures Trials (U)

4 AUTHORS (Last name, first name, middle initial)

Sévigny, Pascale

| 5 DATE OF PUBLICATION (month and year of publication of document) | 6a NO OF PAGES (total containing information Include Annexes, Appendices, etc ) | 6b NO OF REFS (total cited i document) |
|---|---|---|
| Janvier 2002 | 26 | 3 |

7 DESCRIPTIVE NOTES (the category of the document, e g technical report, technical note or memorandum If appropriate, enter the type of report, e g interim, progress, summary, annual or final Give the inclusive dates when a specific reporting period is covered )

Technical Memorandum

8 SPONSORING ACTIVITY (the name of the department project office or laboratory sponsoring the research and development Include the address )

DREO
3701 Carling
Ottawa, Ontario, K1A 0Z4

| 9a PROJECT OR GRANT NO (if appropriate, the applicable research and development project or grant number under which the document was written Please specify whether project or grant) | 9b CONTRACT NO (if appropriate, the applicable number under which the document was written) |
|---|---|
| 1AF12 | |

| 10a ORIGINATOR'S DOCUMENT NUMBER (the official document number by which the document is identified by the originating activity This number must be unique to this document ) | 10b OTHER DOCUMENT NOS (Any other numbers which may be assigned this document either by the originator or by the sponsor) |
|---|---|
| DREO TM 2001-106 | |

11 DOCUMENT AVAILABILITY (any limitations on further dissemination of the document, other than those imposed by security classification)

( x ) Unlimited distribution
( ) Distribution limited to defence departments and defence contractors, further distribution only as approved
( ) Distribution limited to defence departments and Canadian defence contractors, further distribution only as approved
( ) Distribution limited to government departments and agencies, further distribution only as approved
( ) Distribution limited to defence departments, further distribution only as approved
( ) Other (please specify)

12 DOCUMENT ANNOUNCEMENT (any limitation to the bibliographic announcement of this document This will normally correspond to the Document Availability (11) However, where further distribution (beyond the audience specified in 11) is possible, a wider announcement audience may be selected )

UNLIMITED

UNCLASSIFIED

SECURITY CLASSIFICATION OF FORM

DCD03 2/06/87

13 ABSTRACT (a brief and factual summary of the document It may also appear elsewhere in the body of the document itself It is highly desirable that the abstract of classified documents be unclassified Each paragraph of the abstract shall begin with an indication of the security classification of the information in the paragraph (unless the document itself is unclassified) represented as (S), (C), or (U) It is not necessary to include here abstracts in both official languages unless the text is bilingual)

This document presents a model developed to study the impact of multipath interference on jammer performance during Electronic Counter-Measures (ECM) trials against Synthetic Aperture Radars (SARs). The work was motivated by the low grazing angle geometry of the NATO SCI-066 AhrCarSAR trial, where the SAR was driven on a long, high bridge while imaging the valley below.
A simple model of specular reflection was used and analytical formulas were developed to make predictions It was found that the geometry of the AhrCarSAR trial was subject to multipath interference, as are some airborne geometries as well. The analysis of the model showed that the interference of direct and reflected-path pulses results in a chirp with a power modulation determined mainly by the reflection coefficient of the surface near the jammer. For horizontal polarizations, the reflection coefficient approaches 1 and multipath effects can be important. For vertical polarizations however, the reflection coefficient can be significantly less than 1 and multipath effects are weak Since a vertical polarization is used for the AhrCarSAR trial, it was predicted that the performance of the jammer would not be significantly affected by multipath interference.

14 KEYWORDS, DESCRIPTORS or IDENTIFIERS (technically meaningful terms or short phrases that characterize a document and could be h in cataloguing the document They should be selected so that no security classification is required Identifiers such as equipment model designation, trade name, military project code name, geographic location may also be included If possible keywords should be selected frc published thesaurus e g Thesaurus of Engineering and Scientific Terms (TEST) and that thesaurus-identified If it is not possible to select indexing terms which are Unclassified, the classification of each should be indicated as with the title )

Electronic Countermeasures
ECM
Multipath Interference
Synthetic Aperture Radar
SAR

P517607.PDF [Page: 33 of 33]

**Defence R&D Canada**
is the national authority for providing
Science and Technology (S&T) leadership
in the advancement and maintenance
of Canada's defence capabilities.

**R et D pour la défense Canada**
est responsable, au niveau national, pour
les sciences et la technologie (S et T)
au service de l'avancement et du maintien des
capacités de défense du Canada.

*517607
CA020828

DEFENCE R&D DÉFENSE

www.drdc-rddc.dnd.ca